Advances in Geo-Energy Research

Original article

Non-Darcy displacement by a non-Newtonian fluid in porous media according to the Barree-Conway model

Zhaoqin Huang[1], Xiaoyu Zhang[1], Jun Yao[1]*, Yushu Wu[2]

[1]*School of Petroleum Engineering, China University of Petroleum (East China), Qingdao 266580, P. R. China*

[2]*Department of Petroleum Engineering, Colorado School of Mines, Golden, CO 80401, USA*

Abstract: An analytical solution for describing the non-Darcy displacement of a Newtonian fluid by a non-Newtonian fluid in porous media has been developed. The two-phase non-Darcy flow is described using the Barree-Conway model under multi-phase conditions. A power-law non-Newtonian fluid, whose viscosity is a function of the flow potential gradient and the phase saturation, is considered. The analytical solution is similar to the Buckley-Leverett theoretical solution, which can be regarded as an extension of the Buckley-Leverett theory to the non-Darcy flow of non-Newtonian fluids. The analytical results revel how non-Darcy displacement by a non-Newtonian fluid is controlled not only by relative permeabilities but also by non-Darcy flow coefficients as well as non-Newtonian rheological constitutive parameters and injection rates. The comparison among Darcy, Forchheimer and Barree-Conway models is also discussed. For application, the analytical solution is then applied to verify a numerical simulator for modeling multi-phase non-Darcy flow of non-Newtonian fluids.

Keywords: Non-Newtonian fluid, non-darcy flow, barree-conway model, buckley-leverett type solution, two-phase immiscible flow.

1. Introduction

Flow of non-Newtonian fluids in porous media is involved in a wide range of practical applications, such as the penetration of glue in porous substrates, the injection of cement in soils, filtration of polymer solutions, etc. (Sochi, 2010). One of the important applications is the enhanced oil recovery (EOR) process in petroleum engineering, in which many non-Newtonian fluids (jel, polymers, foams, emulsions, etc.) are usually used (Alsofi and Blunt, 2010; Li and Delshad, 2014; Rossen et al., 2011; Wu et al., 1991). Non-Newtonian fluids in porous media exhibit a nonlinear behavior, which does not exist in the flow of Newtonian fluids (Uscilowska, 2008).

Darcy's law has been applied widely to study flow and transport behaviors through porous media (Darcy, 1856). However, the relationship between pressure (or potential) gradient and flow velocity at high flow rates cannot be modelled by Darcys law any more (Bear, 2013; Spivey et al., 2004). There is more evidence that the non-Darcy flow at high flow rates occurs in many subsurface, engineering porous and biological porous flow systems (Schfer and Lohnert, 2006; Vafai, 2010; Wu et al., 2011). Motivated by its importance in practical applications and scientific interest, understandings about the flow behavior at high flow rates have been developed by means of experimental and numerical analysis (Evans et al., 1987; Huang and Ayoub, 2008; Mayaud et al., 2014; Pereira et al., 2006; Vincent et al., 2000; Ye et al., 2014). The Forchheimer equation has been used extensively to describe such high velocity flow (Ergun, 1952; Forchheimer, 1901; Wu, 2001; Wu, 2002), which adds a quadratic flow term to account for high velocity inertial effects. However, the Forchheimer equation has been found to be inadequate for modeling the non-Darcy phenomena over the entire flow velocity range (Barree and Conway, 2004; Barree and Conway, 2009; Ranjith and Viete, 2011; Zhang and Yang, 2014a; Zhang and Yang, 2014b).

Recently, Barree and Conway (2004; 2009) developed a new model for describing the non-Darcy flow based on experimental and field data. The further laboratory researches and analyses (Lai et al., 2012; Lopez-Hernandez, 2007) in-

dicate that the Barree-Conway model can describe the non-Darcy flow behavior from low to high flow rates. This model has been applied to the single- and multi-phase non-Darcy flow analysis in porous media (Al-Otaibi and Wu, 2010; Wu et al., 2011). However, all the existing researches and development are focused on the Newtonian fluids. To our best of knowledge, there are no analytical and numerical solutions available for multi-phase non-Darcy flow of non-Newtonian fluids according to the Barree-Conway model.

In this paper, an analytical solution describing the non-Darcy displacement of a non-Newtonian fluid by a non-Newtonian fluid in porous media has been developed for one-dimensional flow based on the Barree-Conway model. A power-law non-Newtonian fluid is considered in this work. The analysis approach follows upon the classical theory of Buckley and Leverett (Buckley and Leverett, 1942) and our previous works for multiphase non-Newtonian fluid flow and displacement in porous media (Wu et al., 2011; Wu et al., 1991). A general procedure for evaluating the non-Darcy behavior of non-Newtonian fluid displacement is developed, based on the analytical solution, which is similar to the graphic method used in Wu et al. (1991). This work can be regarded as an extension of the Buckley-Leverett theory to the non-Darcy flow of non-Newtonian fluids in porous media.

2. Mathematical model

Consider the flow of two immiscible fluids (one Newtonian fluid and one non-Newtonian fluid) in a homogeneous porous medium. Assume that no interphase mass transfer occurs between the two fluids and ignore dispersion and adsorption effects. The governing equation for fluid is then given by the mass conservation equation,

$$-\bigtriangledown \cdot (\rho_l v_l) + q_l = \frac{\partial}{\partial t}(\rho_l \phi S_t) \tag{1}$$

where ρ_l is the density of fluid l ($l = ne$ for the Newtonian fluid and $l = nn$ for the non-Newtonian fluid), v_l is the flow velocity of fluid l, q_l is the sink/source term of phase l per unit volume of porous media, S_l is the saturation of fluid l, t is time, and ϕ is the effective porosity of porous media.

The flow velocity (volumetric flow rate) in non-Darcy flow for each fluid and its dependence on other parameters need to be defined before the governing equation (1) can be solved. On the basis of experimental data and theoretical analyses (Lai et al., 2012; Lopez-Hernandez, 2007; Wu et al., 2011), the multiphase extension of the Barree-Conway model is used in this work, given by:

$$-\bigtriangledown \Phi_l = \frac{\mu_l v_l}{k_d k_{rl}(k_{mr} + \frac{(1-k_{mr})\mu_l S_l \tau}{\mu_l S_l \tau + \rho_l |v_l|})} \tag{2}$$

where k_d is the constant Darcy or absolute permeability, k_{rl} is the relative permeability to fluid l, μ_l is the dynamic viscosity of fluid l, k_{mr} is the minimum permeability ratio at high rate, relative to Darcy permeability, τ is the inverse of characteristic length, and $\bigtriangledown \Phi_l$ is the potential gradient, defined as:

$$\bigtriangledown \Phi_l = \bigtriangledown p_l - \rho_l g \tag{3}$$

here g is the gravity acceleration vector.

For a power-law non-Newtonian fluid, the relationship of shear stress σ and shear rate γ can be described as follows:

$$\sigma = H\gamma^n \tag{4}$$

where n and H are parameters, called power-law index and consistency of the power-law fluid, respectively. The power-law index is a dimensionless constant, and for pseudo-plastic or shear thinning fluids ranges over $0<n<1$. The consistency H has units (Pa·s^n), depending on the index n. For a Newtonian fluid, $n = 1$ and the viscosity equals the constant H. Apparent viscosity for a power-law fluid is defined as:

$$\mu_{app} = H\gamma^{n-1} \tag{5}$$

For single-phase flow, the modified Blake-Kozeny equation for one-dimensional flow of power-law fluids gives (Bird et al., 2007):

$$v = [\frac{k}{\mu_{eff}}(-\frac{\partial p}{\partial x})]^{\frac{1}{n}} \tag{6}$$

where effective viscosity is defined as:

$$\mu_{eff} = \frac{H}{12}(9 + \frac{3}{n})^n (150k\phi)^{(\frac{1-n}{2})} \tag{7}$$

Equation (6) is the usual flow model used in engineering treatment. Recently, Mikelic (1997) used homogenization theory to derive a nonlinear, one-dimensional power-like law, which is identical to Equation (6). However, Mikelic pointed out that this law could be extended to the N-dimensional ($N > 1$), from an engineering point of view (Mikelic, 1997).

As aforementioned in our previous work (Wu et al., 1991), for the two-phase flow case, we can extend Equation (7) by replacing k by kk_{rl} and ϕ by $\phi(S_{nn} - S_{nnr})$ to obtain:

$$\mu_{eff} = \frac{H}{12}(9 + \frac{3}{n})^n [150kk_{rl}\phi(S_{nn} - S_{nnr})]^{(1-n)/2} \tag{8}$$

In this work, we relate the flow velocity to the pressure gradient as is normally done in multiple-phase extension of non-Darcy flow, with all of the nonlinearities combined into an equivalent non-Newtonian viscosity (Wu et al., 1991). Then, we write:

$$v = -\frac{kk_{rnn}}{\mu_{nn}}\frac{\partial p}{\partial x} \tag{9}$$

This requires the volumetric flux be equal to Equation (6), leading to:

$$\mu_{nn}(S_{nn}, \frac{\partial p}{\partial x}) = \mu_{eff}[\frac{kk_{rnn}}{\mu_{eff}}(-\frac{\partial p}{\partial x})]^{\frac{1}{n}} \tag{10}$$

It should be noted that the Equations (9) and (10) are valid for Darcy flow case. However, the recent research results (Tosco et al., 2013) indicate that the inertial effect and coefficients are demonstrated to be independent of the viscous properties of the fluids, and the above Equation (10) may be directly used in Equation (2).

For capillary pressure and saturation, we still use:

$$p_c(S_{nn}) = p_{ne} - p_{nn} \qquad (11)$$

$$S_{ne} + S_{nn} = 1 \qquad (12)$$

3. Analytical solution

For the derivation of the analytical solution, we assume that the following Buckley-Leverett flow conditions (Wu et al., 2011): (1) Both fluids and the porous medium are incompressible; (2) Capillary pressure gradient and gravity segregation effect are negligible (i.e., stable displacement exists near the displacement front); (3) One-dimensional flow and displacement is along the x coordinate of a length L of linear flow system with a constant cross-sectional area A.

Among these assumptions, incompressibility of fluids and porous media is critical to derive the Buckley-Leverett type solution. This assumption provides a good approximation to displacement processes of two liquids (e.g., oil and water) through porous media, because of the small compressibility of the two fluids as well as rock. For gas and liquid displacement, this assumption may pose certain limitation to the resulting solution, when large pressure gradients build up in a flow system. In many cases, however, this assumption may still provide acceptable approximations because the viscosity of the gas phase in normal reservoir conditions is 2 orders of magnitude lower than the liquid phase. This tends to prevent high-pressure gradients from building up, as in the case of the Buckley-Leverett solution, which was also derived for oil and gas displacement originally.

Considering a one-dimensional problem and ignoring the sink/source term, Equation (1) can then be written as follows:

$$-\frac{\partial v_l}{\partial x} = \phi \frac{\partial S_l}{\partial t} \qquad (13)$$

where v_l is the x-component of seepage velocity or volumetric flow rate (m/s) per unit area of porous media for fluid l . For the one-dimensional flow, v_l can be determined by Equation (2):

$$v_l = -\frac{1}{2\rho_l \mu_l}[\mu_l^2 S_l \tau + \frac{\partial \Phi_l}{\partial x} k_d k_{mr} k_{rl} \rho_l] + \frac{1}{2\rho_l \mu_l} \cdot$$
$$\sqrt{[\mu_l^2 S_l \tau + \frac{\partial \Phi_l}{\partial x} k_d k_{mr} k_{rl} \rho_l]^2 - 4\mu_l^2 S_l \tau \rho_l k_d k_{rl} \frac{\partial \Phi_l}{\partial x}} \qquad (14)$$

where $\frac{\partial}{\partial x}$ is the component of the pressure gradient along x-coordinate, the same for the Newtonian or non-Newtonian fluids since we neglect the capillary gradient term in this work,
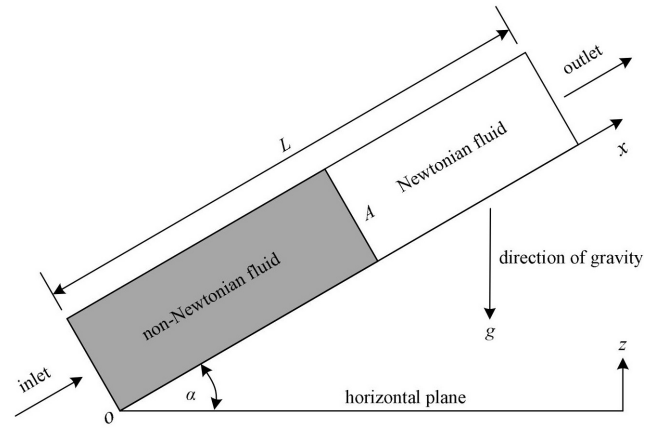

Fig. 1. Schematic of displacement of a Newtonian fluid by a non-Newtonian fluid.

g is the gravitational acceleration constant, and α is the angle between the horizontal plane and the flow direction (i.e. the x-coordinate), as illustrated in Figure 1.

To complete the mathematical model of the physical problem, the initial and boundary conditions must be specified. For simplicity in derivation, the system is initially assumed to be uniformly saturated with both Newtonian and non-Newtonian fluids. The non-Newtonian phase is at its residual saturation, and a Newtonian fluid is at its maximum saturation in the system as follows:

$$S_{ne}(x, t = 0) = 1 - S_{nnr} \qquad (15)$$

where S_{nnr} is the residual non-Newtonian fluid saturation. Non-Newtonian fluid, such as polymer solution, is continuously being injected at a rate, $q(t)$. So, the boundary conditions at the inlet are:

$$v_{nn}(x = 0, t) = \frac{q(t)}{A}, \quad v_{ne}(x = 0, t) = 0 \qquad (16)$$

Following the work of Wu et al., 2011, the fractional flow concept is used to simplify the governing equation (13) in terms of saturation only. The fractional flow is defined as the volume fraction of the phase flowing at a location and time t to the total volume of the flowing phases (Bear, 2013), which can be written as:

$$f_l = \frac{v_l}{v_{nn} + v_{ne}} = \frac{v_l}{v(t)} \qquad (17)$$

From the definition, we have $f_{nn} + f_{ne} = 1$. Equations (10) and (17) indicate that the fractional flow of the displacing non-Newtonian fluid, f_{nn} is generally a function of both saturation and potential gradient. Under the usual simplifications made in the Buckley-Leverett problem, however, the potential gradient is related uniquely to saturation as follows:

$$\frac{q(t)}{A} + \frac{1}{2\rho_{nn}\mu_{nn}}[\mu_{nn}^2 S_{nn}\tau + \frac{\partial \Phi_{nn}}{\partial x} k_d k_{mr} k_{rnn} \rho_{nn}] - \frac{1}{2\rho_{nn}\mu_{nn}}\sqrt{[\mu_{nn}^2 S_{nn}\tau + \frac{\partial \Phi_{nn}}{\partial x} k_d k_{mr} k_{rnn} \rho_{nn}]^2 - 4\mu_{nn}^2 S_{nn}\tau \rho_{nn} k_d k_{rnn} \frac{\partial \Phi_{nn}}{\partial x}}$$
$$+ \frac{1}{2\rho_{ne}\mu_{ne}}[\mu_{nn}^2 S_{nn}\tau + \frac{\partial \Phi_{nn}}{\partial x} k_d k_{mr} k_{rnn} \rho_{nn}] - \frac{1}{2\rho_{ne}\mu_{ne}}\sqrt{[\mu_{ne}^2 S_{ne}\tau + \frac{\partial \Phi_{ne}}{\partial x} k_d k_{mr} k_{rne} \rho_{ne}]^2 - 4\mu_{ne}^2 S_{ne}\tau \rho_{ne} k_d k_{rne} \frac{\partial \Phi_{ne}}{\partial x}} = 0$$

$$(18)$$

Therefore, the fractional-flow function in equation (17) ends up being a function of saturation only, and the Welge graphic method (Welge, 1952) can be applied for evaluation of non-Darcy displacement of immiscible fluids. For a particular saturation of the non-Newtonian fluid, S_{nn}, the corresponding flow potential gradient for the non-Newtonian fluid can be derived by introducing equation (18). The apparent viscosities for the non-Newtonian fluid are determined by use of equation (10), and then the fractional-flow curve can be calculated from equation (17).

The governing equation, (13), subject to the boundary and initial conditions described in Equations (15) and (16), can be solved as follows:

$$\frac{dx}{dt}|_{S_{nn}} = \frac{q(t)}{A\phi} \frac{\partial f_{nn}}{\partial S_{nn}}|_t \qquad (19)$$

This is the frontal advance equation for the non-Darcy displacement of a Newtonian fluid by a non-Newtonian fluid, and it has the same form as the Buckley-Leverett equation. However, the dependence of the fractional flow f_{nn} for the non-Darcy displacement on saturation is different. The fractional flow, f_{nn}, is related to saturation not only through the relative permeability functions, but also through the non-Darcy flow relation and non-Newtonian rheology constitutes, as described by Equations (2) and (10).

For a given time and a given injection rate, Equation (19) indicates that a particular non-Newtonian fluid saturation profile propagates through the porous medium at a constant velocity. As in the Buckley-Leverett theory, the saturation for a vanishing capillary pressure gradient will, in general, become a multiple-valued function of distance near the displacement front (Cardwell, 1959). Equation (19) will then fail to describe the velocity of the shock saturation front since $\partial f_{nn}/\partial S_{nn}$ does not exist on the front, because of the discontinuity in S_{nn} at that point. Consideration of mass balance across the shock front, Sheldon and Cardwell (1959) provides the velocity of the front:

$$\frac{dx}{dt}|_{S_{nnf}} = \frac{q(t)}{A\phi} \frac{f_{nn}^+ - f_{nn}^-}{S_{nn}^+ - S_{nn}^-} \qquad (20)$$

where S_{nnf} is the shock front saturation of the displacing non-Newtonian fluid. The plus and minus superscripts refer to values immediately ahead of and behind the shock front, respectively.

The location x of any saturation S_{nn} traveling from the inlet at time t can be determined by integrating equation (19) with respect to time, which leads to:

$$xS_{nn} = \frac{1}{A\phi} \int_0^t q(t) \frac{\partial f_{nn}}{\partial S_{nn}}|_{S_{nn}} dt \qquad (21)$$

For a given injection rate, $q(t)$, the derivative $\partial f_{nn}/\partial S_{nn}$ within the integral is also a time-dependent function. Therefore, the solution (21) for non-Darcy displacement of non-Newtonian fluid differs from the Buckley-Leverett solution.

Considering a constant injection rate, then Equation (21) becomes:

$$xS_{nn} = \frac{q(t)}{A\phi} \frac{\partial f_{nn}}{\partial S_{nn}}|_{S_{nn}} \qquad (22)$$

where q is the constant injection rate, and $q(t)$ is the cumulative volume of the injected fluid.

For given x and t, using Equation (22) will result in a multiple-valued saturation distribution, which can be handled by a mass balance calculation, as in the Buckley-Leverett solution. An alternative Welge graphic method (Welge, 1952) can be shown to apply to calculating the above solution in this case. The only additional step in applying this method is to take into account the contribution of the pressure gradient dependence on the non-Newtonian viscosity and non-Darcy coefficient, using a fractional flow curve. Then the non-Newtonian fluid saturation at the shock front can be obtained by:

$$\frac{\partial f_{nn}}{\partial S_{nn}}|_{S_{nnf}} = \frac{f_{nn}(S_{nnf}) - f_{nn}(S_{nnr})}{S_{nnf} - S_{nnr}} \qquad (23)$$

Then, the complete saturation profile can be determined using Equation (22).

4. Results and discussion

In this section, the analytical solution presented above is used to give us some insight into non-Darcy flow and displacement phenomena of non-Newtonian fluids. Initially, the one-dimensional linear porous medium system is assumed to be saturated with only a Newtonian fluid, and a non-Newtonian fluid is injected at a constant volumetric rate at the inlet, $x = 0$, starting from $t = 0$. The relative permeabilities are given as power-law functions of saturation similar to the Brooks-Corey curves (Alpak et al., 1999):

$$k_{rnn} = k_{rnn,max}(\frac{S_{nn} - S_{nnr}}{1 - S_{nnr} - S_{nnr}})^{n_{nn}} \qquad (24)$$

$$k_{rne} = k_{rne,max}(\frac{1 - S_{nn} - S_{ner}}{1 - S_{nnr} - S_{ner}})^{n_{ne}} \qquad (25)$$

where $k_{rl,max}$ is the maximum relative permeability of fluid l, n_l is the exponents of fluid l.

4.1 Effects of non-Darcy parameters

For a given constant injection rate, the solution (22) shows that non-Darcy non-Newtonian fluid displacement in a porous medium is characterized not only by relative permeability data, as in Buckley-Leverett displacement, but also by non-Darcy flow coefficients and non-Newtonian fluid parameters. Using the analytical solution, some fundamental aspects of non-Darcy displacement will be shown. Figure 2 shows the relative permeability curves. The fluid and rock properties are summarized in Table 1.

Table 1. Parameters for the non-Darcy displacement examples.

Parameters	Value	Unit
Porosity, ϕ	0.3	[-]
Absolute permeability, k_d	9.86910-12	$[m^2]$
Minimum permeability, k_{mr}	0.001	[-]
Inverse of characteristic length, τ	10^3	[1/m]
Cross-section area, A	1.0	$[m^2]$
Injection rate, q	1.010^{-3}	[1/m]
Injection time, t	0.1	[hours]
Viscosity of Newtonian fluid, μ_{ne}	5.0	$[mPa*s]$
Power-law index, n	0.6	[-]
Consistency of power-law fluid, H	0.01	$[Pa*s^n]$
Residual fluid saturations, S_{ner}, S_{nnr}	0.2, 0.2	[-]
Power index of relative permeability function, n_{ne}, n_{nn}	2.0, 2.0	[-]
Maximum relative permeability of fluids, $k_{rne,max}, k_{rnn,max}$	0.75, 0.75	[-]
Density of Newtonian fluid, ρ_{ne}	800	$[kg/m^3]$
Density of non-Newtonian fluid, ρ_{nn}	1000	$[kg/m^3]$
Directional angle, α	0	[rad]

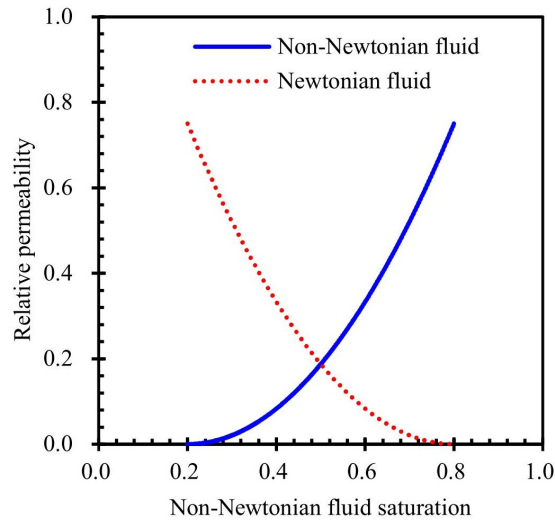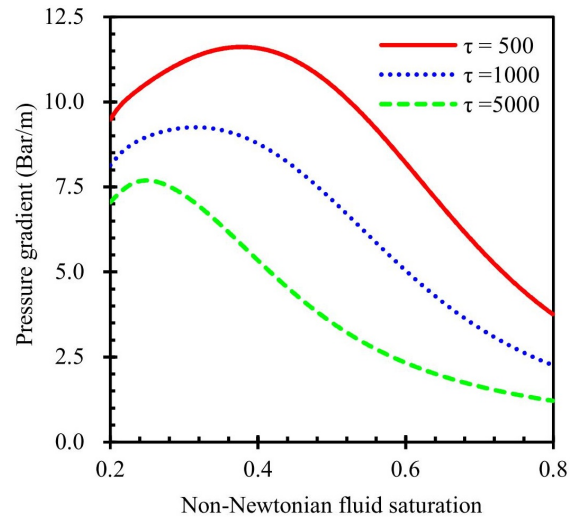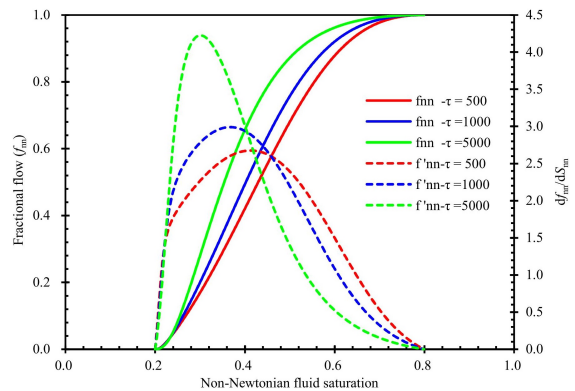**Fig. 2.** Relative permeability curves.

Fig. 3. Pressure gradients with different parameter, τ.

Figure 3, obtained by using Equation (18), shows that pressure gradients change significantly as a function of saturation for different non-Darcy parameter, τ. At both high and low values for the non-Newtonian fluid saturation, the pressure gradients become relatively small, because the total flow resistance decreases as the flow is close to single-phase flow condition. In addition, Figure 3 indicates that as the non-Darcy flow parameter τ decreases, the pressure gradient increases at the same saturation value under the same injection rate due to a larger non-Darcy flow term effect. However, Equation (2) indicates that the pressure (or potential) gradient is a comprehensive function of non-Darcy parameters, τ and

Fig. 4. Fractional flow curves and their derivatives with respect to non-Newtonian fluid saturation for different non-Darcy flow parameter τ.
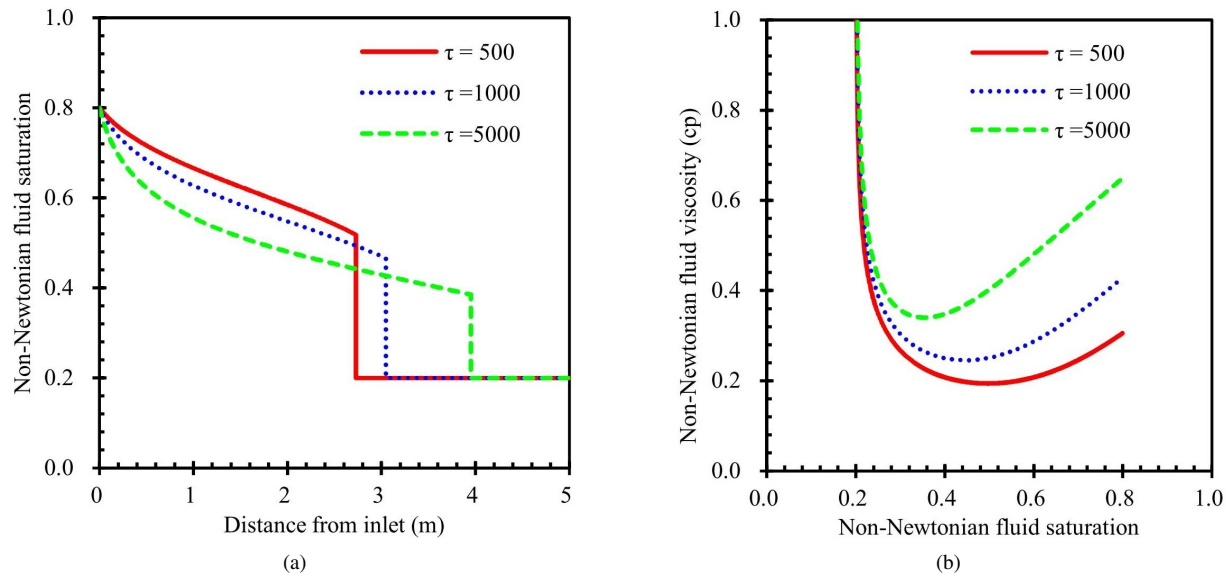
Fig. 5. (a) Non-Newtonian Saturation profiles with different model parameter τ after 0.1-hours injection; (b) effects of the non-Darcy flow parameter τ on non-Newtonian fluid apparent viscosity.
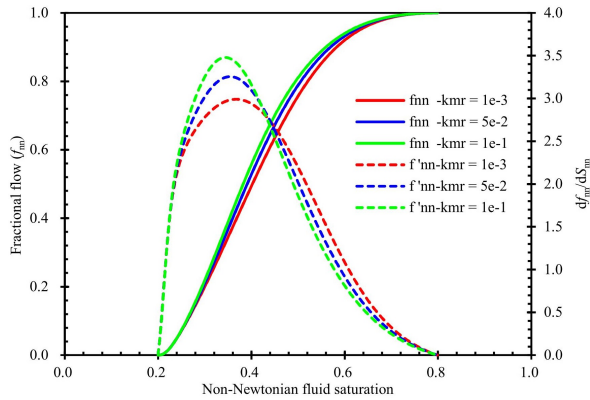

Fig. 6. Fractional flow curves and their derivatives with respect to non-Newtonian fluid saturation for different non-Darcy flow constant k_{mr}.

k_{mr}, and non-Newtonian fluid viscosity μ_{nn}, which is also a function of pressure gradient.

The resulting fractional flow curves and their derivatives with different non-Darcy parameter τ are shown in Figure 4. Note that fractional flow curves change with the non-Darcy flow parameter τ due to the change in pressure gradient under the same saturation. Non-Newtonian fluid saturation profiles of displacement after 0.1-hours injection period are plotted in Figure 5-a. In terms of higher sweeping efficiency or shorter displacement front travel distance, a smaller non-Darcy flow parameter τ leads to higher non-Newtonian fluid displacing flow rates. This results in a better displacement efficiency: more Newtonian fluid is displaced from the swept zone. Moreover, the displacement becomes the Buckley-Leverett process as the non-Darcy flow parameter, τ, becomes large. The effect of non-Darcy flow parameter τ on non-Newtonian fluid apparent viscosity is shown in Figure 5-b, in which a constant power index (n=0.6) of non-Newtonian fluid viscosity is used. Figure 5-b indicates that non-Newtonian fluid

apparent viscosity may be very sensitive to non-Darcy flow parameter, τ.

Figures 6 and 7 present results for sensitivity of non-Darcy parameter k_{mr}. The resulting fractional flow curves and their derivatives with different non-Darcy parameter k_{mr} are shown in Figure 6. As shown in the Figures 4 and 6, fractional flow curves change also with the non-Darcy model parameters under the same saturation. Figure 7-a presents the non-Newtonian fluid saturation profiles of non-Darcy displacement with varying k_{mr}. It shows that a smaller non-Darcy flow parameter k_{mr} leads to higher non-Newtonian fluid displacing flow rates because of a larger non-Darcy flow term effect. Figure 7-b shows the effect of non-Darcy flow parameter k_{mr} on non-Newtonian fluid apparent viscosity. Figures 3~7 also indicate that the Barree-Conway model results are more sensitive to the parameter τ than k_{mr}, from the parameters selected.

4.2 Effects of injection rates

Figure 8, obtained using Equations (14) and (17), shows that both all the fractional flow and its derivatives change significantly with varying injection rates for horizontal displacement system. The fluid and rock properties are the same as Table 1, except the non-Darcy flow parameters τ and k_{mr}. The effects of injection rates on non-Darcy displacement is shown in Figure 9-a, in which constant non-Darcy flow parameters, $\tau = 500$ and $k_{mr}= 0.001$, are used with all three injection rates. Figure 9-a indicates that non-Darcy displacements of non-Newtonian fluid are also sensitive to injection rates. This rate-dependent displacement behavior is entirely different from a Buckley-Leverett or Darcy displacement, because the latter is independent of injection rates.

Under non-Darcy flow condition, Figure 9-a shows that for the same volume of water injected with the three injection rates, saturation profiles in the system are very different. Lar-
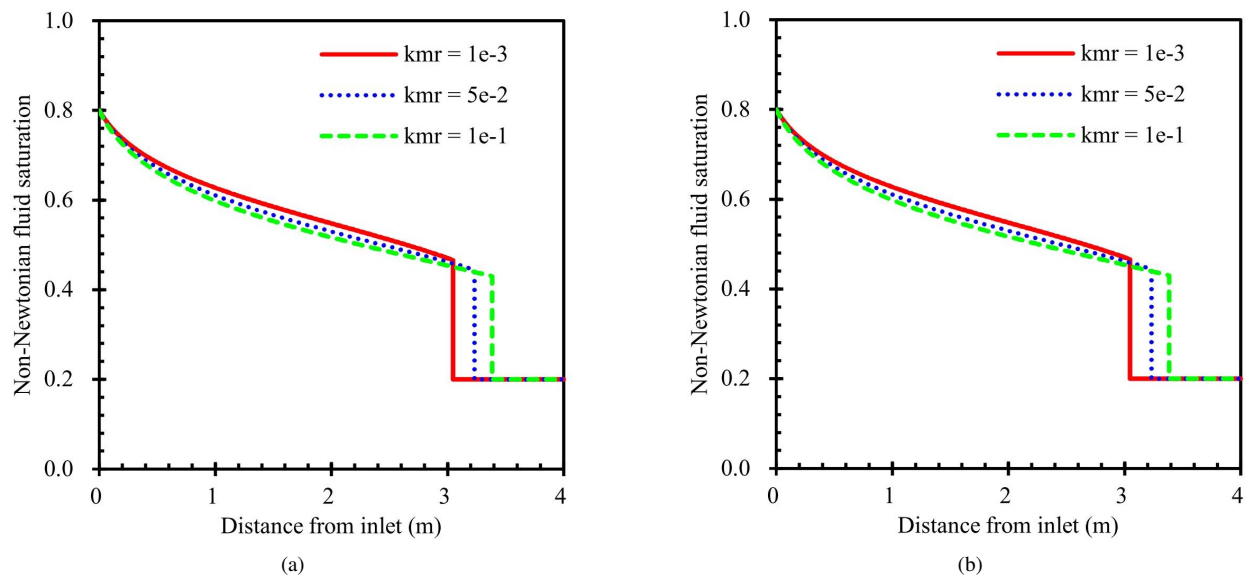
Fig. 7. (a) Non-Newtonian Saturation profiles with different model parameter k_{mr} after 0.1-hours injection; (b) effects of the non-Darcy flow parameter k_{mr} on non-Newtonian fluid apparent viscosity.
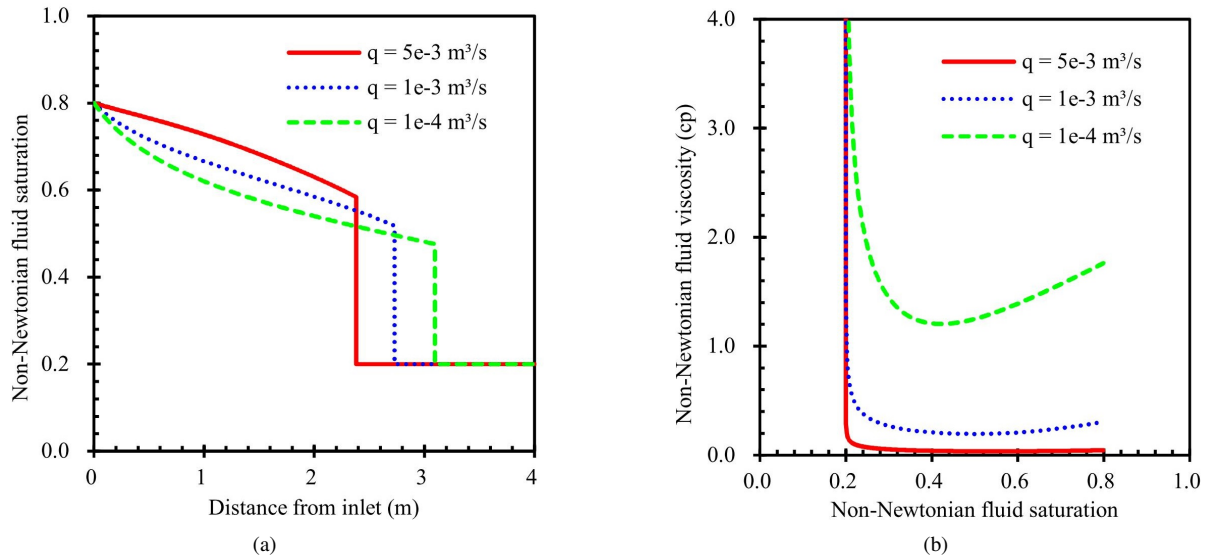

Fig. 9 . (a) Saturation profiles with different injection rates after injection of 0.36 m^3 non-Newtonian fluid; (b) effects of the injection rates on non-Newtonian fluid apparent viscosity.
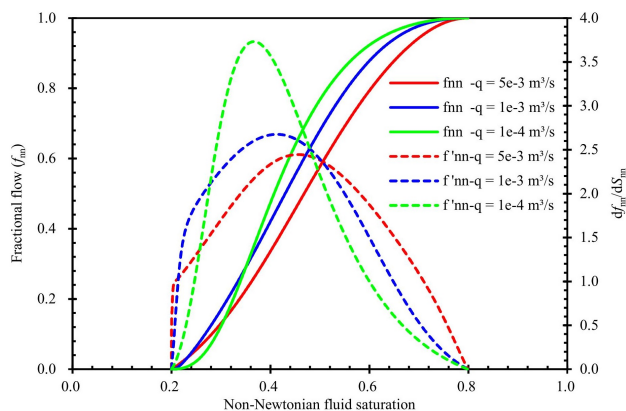

Fig. 8 . Fractional flow curves and their derivatives with respect to non-Newtonian fluid saturation for different injection rates.

ger injection rates display better sweeping efficiency overall. This is because higher injection rates create larger flow resistance to the displacing phase due to the non-Darcy term, and as a result this will lower flow velocity of the displacing phase, relative to that of the displaced phase, resulting in a better sweeping performance. Figure 9-b indicates the apparent viscosity of non-Newtonian fluid is sensitive to the injection rate.

4.3 Effects of non-Newtonian fluid parameters

There are two parameters that characterize the flow behavior of a power-law fluid, the exponential index, n, and consistency parameter, H. For a pseudoplastic fluid, $0<n<1$. If $n = 1$, the fluid is Newtonian. The effect of the power-law index, n,
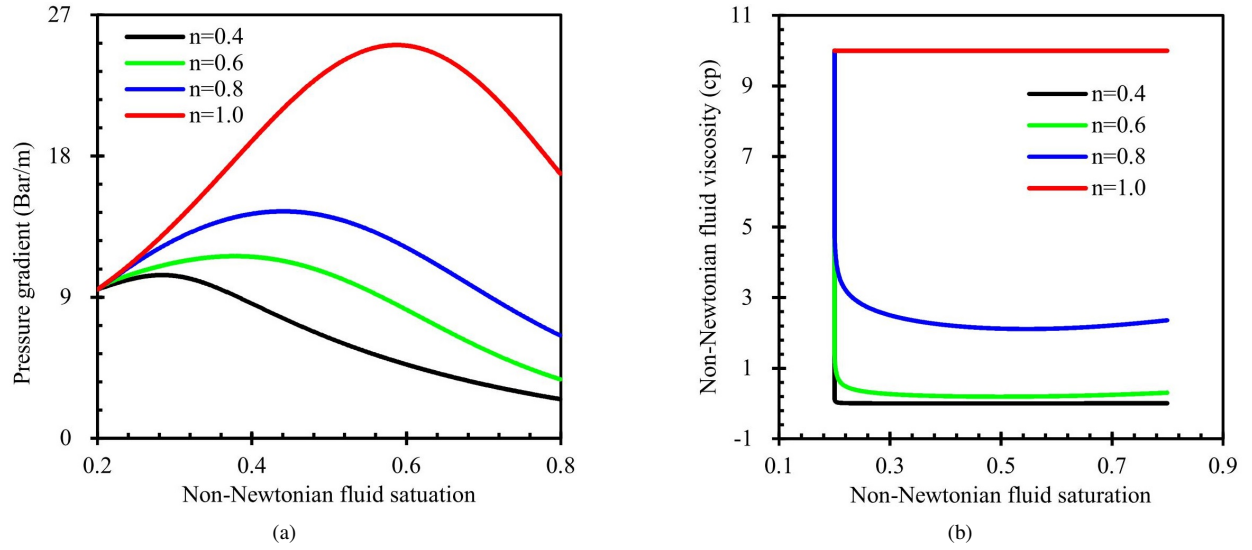
Fig. 10. Effects of the power-law index on pressure gradients (a); Effects of the power-law index on apparent viscosity of non-Newtonian fluid (b).
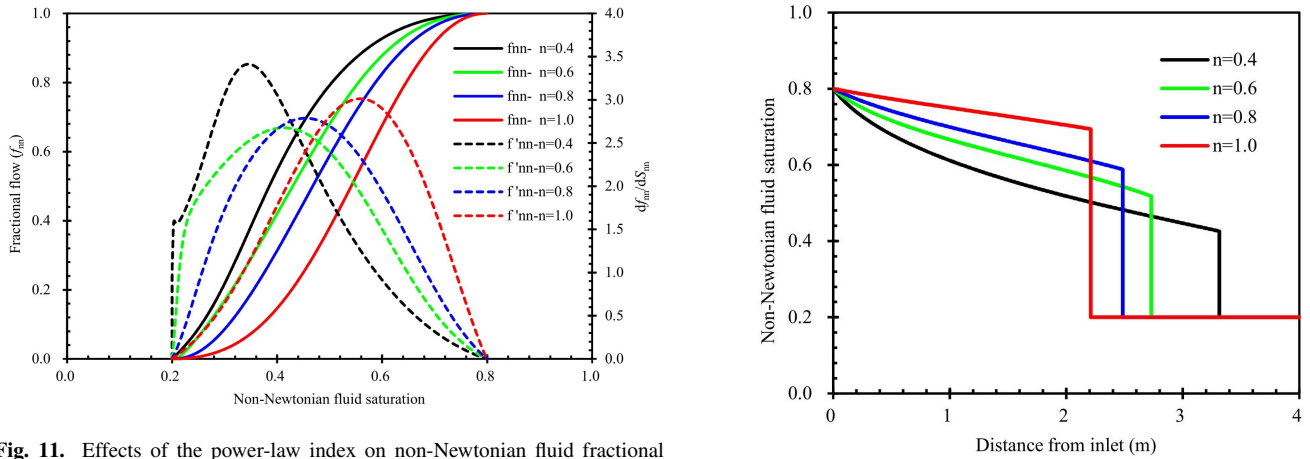

Fig. 11. Effects of the power-law index on non-Newtonian fluid fractional flow curve and its derivatives.

Fig. 12. Effects of the power-law index on non-Newtonian fluid saturation profiles.

on horizontal displacement can be quite significant. Figure 10-a shows that the pressure gradients are changed largely as a function of saturation for different n. The apparent viscosities of several non-Newtonian fluids are given in Figure 10-b, and the resulting fractional flow curves are shown in Figure 11. In all these analysis, constant non-Darcy flow parameters, $\tau = 500$ and $k_{mr} = 0.001$, and a constant injection rate, $q = 1.010\text{-}3$ m^3/s, are used with all different power-law indexes. The other fluid and rock parameters have been listed in Table 1.

Saturation profiles after 0.1-hours injection period in the system are plotted in Figure 12. Note the significant differences in sweep efficiency. Since the power-law index, n is usually determined from an experiment or from well test analysis, some errors cannot be avoided in determining the value of n because of the extreme sensitivity of the core saturation distribution to n. The sensitivity of the displacement behavior to the power-index n suggests that in determining the index n, it may be helpful to match experimental saturation profiles using the analytical solution.

4.4 Comparison between Barree-Conway and Forchheimer models

The equivalent Forchheimer non-Darcy parameters can be evaluated from the Barree-Conway model input parameters (wu et al., 2011). A multiphase extension of the Forchheimer model can be described as follows (Wu, 2001):
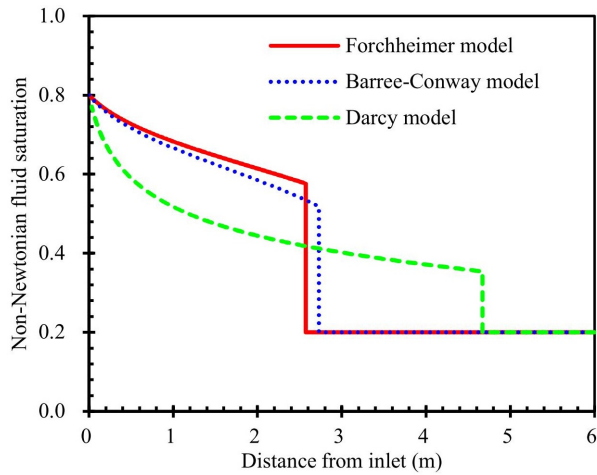
$$- \bigtriangledown \Phi_l = \frac{\mu_l}{k_d k_{rl}} v_l + \beta_l \rho_l v_l |v_l| \qquad (26)$$

where β_l is the non-Darcy flow parameter for fluid l under multi-phase flow conditions, and it is given as:

$$\beta_l(S_l, k_{rl}) = \frac{C_\beta}{(k_d k_{rl})^{5/4} [\phi(S_l - S_{lr})]^{3/4}} \qquad (27)$$

Table 2. Parameters for the non-Darcy displacement comparison example.

Parameters	Value	Unit
Porosity, ϕ	0.3	[-]
Absolute permeability, k_d	9.869×10^{-12}	$[m^2]$
Minimum permeability, k_{mr}	0.001	[-]
Inverse of characteristic length, τ	5×10^2	[1/m]
Cross-section area, A	1.0	$[m^2]$
Injection rate, q	1.010^{-3}	$[m^3/s]$
Injection time, t	0.1	[hours]
Viscosity of Newtonian fluid, μ_{ne}	5.0	[mPas]
Power-law index, n	0.6	[-]
Consistency of power-law fluid, H	0.01	$[Pas^n]$
Equivalent non-Darcy flow constant, C_β	1.435×10^{-6}	$[m^{3/2}]$
Density of Newtonian fluid, ρ_{ne}	800	$[kg/m^3]$
Density of non-Newtonian fluid, ρ_{nn}	1000	$[kg/m^3]$
Directional angle, α	0	[rad]

Fig. 13. Comparison of the results from Darcy, Forchheimer, and Barree-Conway models.

where C_β is a non-Darcy flow constant with a unit of meters$^{3/2}$ if converted to SI units. From Equations (2) and (27), we can solve non-Darcy parameter β_l in term of Barree-Conway input parameters:

$$\beta_l = \frac{\mu_l(1 - k_{mr})}{k_d k_{rl}(k_{mr}\rho_l|v_l| + \mu_l S_l \tau)} \quad (28)$$

And then, we can calculate the non-Darcy constant, C_β, according to the single-phase case in Equations (27) and (28), which is given by:

$$C_\beta = \frac{\mu_l(1 - k_{mr})(k_d)^{5/4}\phi^{3/4}}{k_d k_{rl}(k_{mr}\rho_l|v_l| + \mu_l \tau)} \quad (29)$$

Figure 13 shows a comparison among Darcy, Forchheimer non-Darcy, and Barree-Conway non-Darcy models. The corresponding calculation parameters are summarized in Table 2. The relative permeability parameters are the same as Table

1. Note that to compare the results from the two non-Darcy models, equivalent non-Darcy flow parameter C_β are used for the Forchheimer and Barree-Conway models. As shown in Figure 13, the two non-Darcy models, when using the equivalent non-Darcy flow parameters, present similar behavior where non-Darcy effect decreases the frontal velocity, and the slight discrepancy between the two non-Darcy models appear to be minimal. Actually, the equivalent non-Darcy flow parameter C_β should also be a function of saturation according to Equations (27) and (28). However, the non-Darcy flow parameter C_β is constant in Forchheimer model. This is the main cause of slight difference between Forchheimer and Barree-Conway models results. Nevertheless, the difference between the non-Darcy and Darcy displacement seems large.

4.5 Verification of numerical model

In this section, the analytical solutions are used to examine the validity of the numerical method implemented in a general purpose, three-phase reservoir simulator, the MSFLOW code (Wu, 1998 and 2015), for modeling multiphase non-Newtonian flow and displacement processes according to the Barree-Conway model, i.e. Equation (2) (Wu et al., 2011). To reduce the effects of discretization on numerical simulation results, very fine, uniform mesh spacing ($\triangle x=$ 0.01 m) is chosen. A one-dimensional 5-m linear domain is discretized into 500 one-dimensional grid blocks.

The flow description and the parameters for this problem are illustrated in Table 3. The relative permeability parameters are the same as Table 1. In the numerical simulation the non-Darcy flow flux, Equation (14), is estimated using a full upstream weighting scheme as that for the relative permeability function. The comparison between the numerical and analytical solutions is shown in Figure 14. Figure 14 indicates that the numerical results are in excellent agreement with the analytical solutions of the non-Darcy displacement for
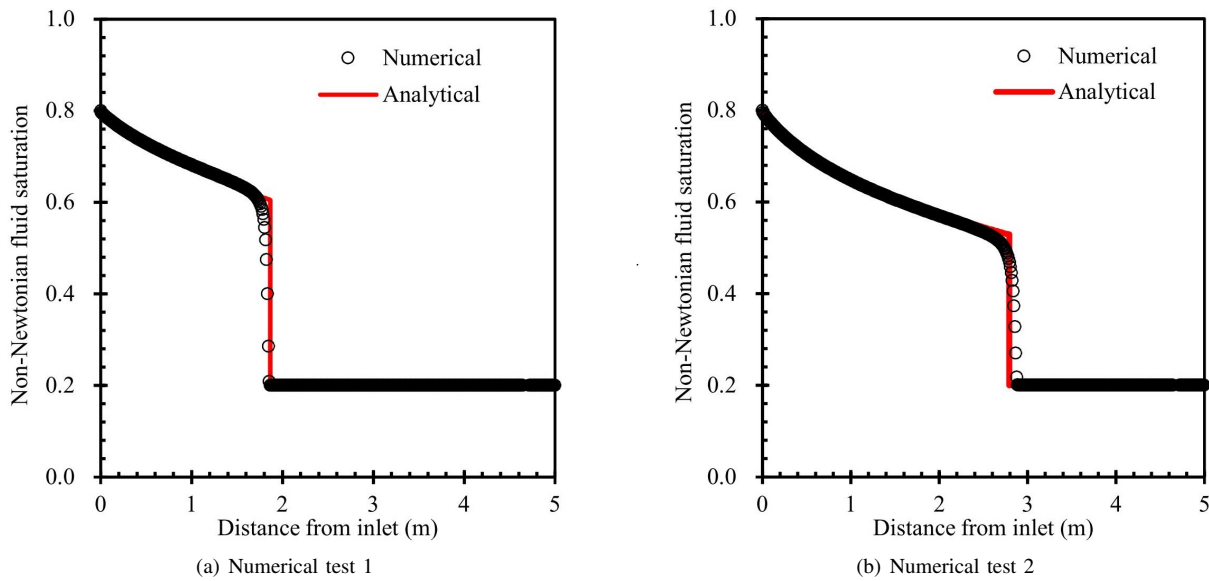
(a) Numerical test 1

(b) Numerical test 2

Fig. 14. Comparison between analytical and numerical solutions after 10 hours of injection, the corresponding fluid and rock properties are listed in Table 2.

Table 3. Fluid and rock properties for comparing analytical and numerical solutions.

Parameters	Numerical test 1	Numerical test 2	Unit
Porosity, ϕ	0.4	0.3	[-]
Absolute permeability, k_d	9.869×10^{-13}	9.869×10^{-13}	$[m^2]$
Minimum permeability, k_{mr}	0.1	0.1	[-]
Inverse of characteristic length, τ	0.5×10^3	1.0×10^3	[1/m]
Cross-section area, A	1.0	1.0	$[m^2]$
Injection rate, q	1.010^{-5}	1.010^{-5}	$[m^3/s]$
Injection time, t	10.0	10.0	[hours]
Viscosity of Newtonian fluid, μ_{ne}	6.0	5.0	[mPas]
Power-law index, n	0.8	0.6	[-]
Consistency of power-law fluid, H	0.01	0.01	$[Pas^n]$
Density of Newtonian fluid, ρ_{ne}	800	800	$[kg/m^3]$
Density of non-Newtonian fluid, ρ_{nn}	1000	1000	$[kg/m^3]$
Directional angle, α	0	0	[rad]

the entire non-Newtonian phase sweeping zone. Except at the shock front, the numerical solutions deviate only slightly from the analytical solutions, resulting from a typical smearing front phenomenon of numerical dispersion effects when matching the Buckley-Leverett solution using numerical results (Aziz and Settari, 1979). Considering the complexity introduced when non-Newtonian fluid non-Darcy flow is involved in a multi-phase flow problem, the results from Figure 14 provide a very encouraging indication that our numerical model is correct in describing the multi-phase immiscible displacement of non-Darcy and non-Newtonian fluid flow in porous media.

5. Conclusions

An analytical solution for describing the non-Darcy displacement of a Newtonian fluid by a non-Newtonian fluid through porous media, according to the Barree-Conway model has been developed. A general power-law viscosity function for a non-Newtonian fluid is proposed and used in the solution, which relates non-Newtonian fluid viscosity to the local pressure (or potential) gradient and saturation. The two-phase non-Darcy flow is described using the Barree-Conway model. The analytical solution, derived in this work, is based on the same assumptions as those used for the Buckley-Leverett solution.

The analytical results are used to obtain some insight into the physics of non-Darcy displacement involving non-Newtonian fluid. The solution reveals that non-Darcy displacement by a non-Newtonian fluid is a more complicated process than the Darcy displacement described by the Buckley-Leverett solution and the non-Darcy displacement of a Newtonian fluid. Two-phase non-Darcy flow and displacement are controlled not only by relative permeability curves, such as in Darcy displacement, but also by non-Darcy flow parameters

as well as non-Newtonian rheological constitutive and injection rates. The comparison between Forchheimer and Barree-Conway models indicates a similar flow behavior observed, which is very different from prediction of Darcy model.

Furthermore, the analysis procedure in this work can be easily extended to other one-dimensional geometries, such as radial or composite systems. In addition, the analytical solution is also applicable to displacement processes involving other non-Darcy flow models and other non-Newtonian rheological constitutive models, such as Bingham-, Cross- and Carreau-type fluids.

Acknowledgments

References

Al-Otaibi, A.M. and Wu, Y.S. Transient behavior and analysis of non-Darcy flow in porous and fractured reservoirs according to the Barree and Conway model. SPE Western Regional Meeting, Anaheim, California, USA, 27-29 May, 2010.

Alpak, F.O., Lake, L.W. and Embid, S.M. Validation of a modified Carman-Kozeny equation to model two-phase relative permeabilities. SPE Annual Technical Conference and Exhibition, Houston, Texas, 3-6 October, 1999.

Alsofi, A.M., Blunt, M.J. Streamline-based simulation of non-Newtonian polymer flooding. SPE J. 2010, 15(4): 895-905.

Aziz, K., Settari, A. Petroleum reservoir simulation. London: Chapman & Hall, 1979.

Barree, R., Conway, M. Beyond beta factors: A complete model for Darcy Forchheimer and trans-Forchheimer flow in porous media. J. Petrol. T. 2005, 57(8): 73.

Barree, R.D., Conway, M. Multiphase non-Darcy flow in proppant packs. SPE Prod. Oper. 2009, 24(2): 257-268.

Bear, J. Dynamics of fluids in porous media. Courier Dover Publications, 2013.

Bird, R.B., Stewart, W.E. and Lightfoot, E.N. Transport phenomena. New Jersey, USA: John Wiley & Sons, 2007.

Buckley, S., Leverett, M. Mechanism of fluid displacement in sands. Transactions of the AIME 1942, 146(1): 107-116.

Cardwell, W. The meaning of the triple value in noncapillary Buckley-Leverett theory. Presented at the 2009 Rocky Mountain Petroleum Technology Conference, Denver, CO, 14-16 April, 2009.

Darcy, H. Les fontaines publiques de la ville de Dijon. Victor

Dalmont, 1856.

Ergun, S. Fluid flow through packed columns. Chem. Eng. Prog. 1952, 48: 89-94.

Evans, R., Hudson, C. and Greenlee, J. The effect of an immobile liquid saturation on the non-Darcy flow coefficient in porous media. SPE Pro. Eng. 1987, 2(4): 331-338.

Forchheimer, P. Wasserbewegung durch boden. Z. Ver. Deutsch. Ing. 1901, 45: 1782-1788.

Huang, H., Ayoub, J.A. Applicability of the Forchheimer equation for non-Darcy flow in porous media. SPE J. 2008, 13(31): 112-122.

Lai, B., Miskimins, J.L., Wu, Y.S., et al. Non-Darcy porous-media flow according to the Barree and Conway model: Laboratory and numerical-modeling studies. SPE J. 2012, 17(1): 70-79.

Li, Z., Delshad, M. Development of an analytical injectivity model for non-Newtonian polymer solutions. SPE J. 2014, 19(3): 381-389.

Lopez-Hernandez, H.D. Experimental analysis and macroscopic and pore-level flow simulations to compare non-Darcy flow models in porous media. Colorado School of Mines. Arthur Lakes Library, 2007.

Mayaud, C., Walker, P., Hergarten, S., et al. Nonlinear flow process: A new package to compute nonlinear flow in MODFLOW. Groundwater 2015, 53(4): 645-650.

Mikelic, A. Non-Newtonian flow, in Homogenization and porous media. SpringerPlus 2007: 77-94.

Pereira, C.A., Kazemi, H. and Ozkan, E. Combined effect of non-Darcy flow and formation damage on gas well performance of dual-porosity and dual-permeability reservoirs. SPE Reserv. Eval. Eng. 2006, 9(5): 543-552.

Ranjith, P., Viete, D. Applicability of the cubic law for non-darcian fracture flow. J. Petrol. Sci. Eng. 2011, 78(2): 321-327.

Rossen, W., Venkatraman, A., Johns, R., et al. Fractional flow theory applicable to non-Newtonian behavior in eor processes. Transp. Porous Med. 2011, 89(2): 213-236.

Schäfer, P., Lohnert, G. Boiling experiments for the validation of dryout models used in reactor safety. Nucl. Eng. Des. 2006, 236(14): 1511-1519.

Sheldon, J., Cardwell, W. One-dimensional incompressible noncapillary. two-phase fluid flow in a porous medium. 1959, 216: 290-296.

Sochi, T. Flow of non-Newtonian fluids in porous media. J. Polym. Sci. Pol. Phys. 2010, 48(23): 2437-2767.

Spivey, J., Brown, K., Sawyer, W., et al. Estimating non-Darcy flow coefficient from buildup-test data with wellbore storage. SPE Reserv. Eval. Eng. 2004, 7(4): 256-269.

Tosco, T., Marchisio, D.L., Lince, F., et al. Extension of the Darcy-Forchheimer law for shear-thinning fluids and validation via pore-scale flow simulations. Transp. Porous Med. 2013, 96(1): 1-20.

Uscilowska, A. Non-Newtonian fluid flow in a porous medium. J. Mech. Mater. Struct. 2008, 3(6): 1151-1159.

Vafai, K. Porous media: applications in biological systems and biotechnology. Florida, USA: CRC Press, 2010.

Vincent, M.C., Pearson, C.M. and Kullman, J. Non-Darcy and multiphase flow in propped fractures: case studies illus-

trate the dramatic effect on well productivity. SPE/CERI gas technology symposium. 2000: 71-84.

Welge, H.J. A simplified method for computing oil recovery by gas or water drive. J. Petrol. T. 1952, 4(4): 91-98.

Wu, Y. MSFLOW: Multiphase subsurface flow model of oil, gas and water in porous and fractured media with water shut-off capability, documentation and users guide. Documentation and Users Guide Walnut Creek, California, 1998.

Wu, Y.S. Non-Darcy displacement of immiscible fluids in porous media. Water Resour. Res. 2001, 37(12):2943-2950.

Wu, Y.S. Numerical simulation of single-phase and multiphase non-Darcy flow in porous and fractured reservoirs. Transp. Porous Med. 2002, 49(2): 209-240.

Wu Y.S. Multiphase fluid flow in porous and fractured reservoirs. Gulf Professional Publishing, 2015.

Wu, Y.S., Lai, B., Miskimins, J.L., et al. Analysis of multiphase non-Darcy flow in porous media. Transp. Porous Med. 2011, 88(2): 205-223.

Wu, Y.S., Pruess, K. and Witherspoon, P. Displacement of a Newtonian fluid by a non-Newtonian fluid in a porous medium. Transp. Porous Med. 1991, 6(2): 115-142.

Ye, Z., Chen, D. and Wang, J. Evaluation of the non-Darcy effect in coalbed methane production. Fuel 2014, 121: 1-10.

Zhang, F., Yang, D. Determination of minimum permeability plateau and characteristic length in porous media with non-Darcy flow behavior. J. Petrol. Sci. Eng. 2014a, 119(0): 8-16.

Zhang, F., Yang, D.T. Determination of fracture conductivity in tight formations with non-Darcy flow behavior. SPE J. 2014b, 19(1): 34-44.